Comparative Analysis of First-Order, Second-Order, and Fourth-Order Low-Pass Filters in Amplitude Modulation Synchronous Demodulation Systems

Gujiacheng Tang

202383890021@nuist.edu.cn

NUIST Waterford Institute, Nanjing University of Information Science and Technology, Nanjing, Jiangsu, 210044, China

Abstract. Amplitude Modulation (AM) is both a ubiquitous modern communication technology and is used extensively in the low-power Internet of Things (IoT). In real-life settings, noise in a channel, system flaws, and electromagnetic interference are major factor that plagues the quality of communications, and this aspect requires proper filtering in order to obtain sound data recovery. The paper explores the behaviour of filters of different orders in an AM synchronous demodulation system. The simulation model includes the amplitude modulation, additive white and pink noise, phase-locked loop synchronous demodulation, and parallel low-pass filtering. Filter performance under the same system parameters is compared using gain accuracy, phase delay time, signal-to-noise ratio (SNR), carrier rejection ratio, total harmonic distortion (THD), and steady state error. Findings show that superior noise suppression, which enhances signal reliability, is attained at higher-order filters, which are susceptible to phase delay and sensitivity in terms of synchronization.

Keywords: AM synchronous demodulation; Butterworth low-pass filter; Filter comparison; Noise suppression; Internet of Things communication

1 Introduction

Efficient and reliable signal recovery technology is the basic requirement in the communication system, especially in the front-end application of the Internet of Things. Communication equipment is often limited by low power consumption, limited hardware resources, and cost requirements. Under such harsh conditions, the communication system is extremely vulnerable to noise from electronic components, environmental interference, electromagnetic coupling, and other factors, which will significantly reduce signal fidelity and data reliability. Although amplitude modulation is one of the earliest modern communication modulation technologies, it still plays an irreplaceable role in simple wireless communication and IT-oriented communication due to its low complexity and high [1]. In the Amplitude Modulation receiving terminal adopting synchronous demodulation, the low-pass filter is an important stage to

ICMEEA 2026, April 24-26, Singapore, Singapore

DOI 10.4108/eai.24-4-2026.2364975

suppress high frequency component and recover the baseband information. Butterworth filters are widely used in various low-pass filter types because their frequency response curves in the passband are maximally flat and their performance is stable [2]. For AM synchronous demodulation systems, the order of the low-pass filter plays a decisive role in determining the attenuation characteristics, phase delay, and system complexity. Therefore, the comparison and analysis of first-order, second-order, and higher-order low-pass filters are of great significance for understanding the standard trade-offs and aiding in the design of reliable and efficient Internet of Things system communication systems.

Previous research has established the theoretical basis for AM modulation and synchronous demodulation, and has thoroughly analyzed their spectral characteristics and the ideal conditions for signal recovery [3]. Li developed a variable projection order Ekblom norm-promoted adaptive algorithm, which showed that increasing the filter order leads to a steeper attenuation slope and enhanced noise suppression [4]. Meanwhile, B.T.Krishna proposed two active implementation methods for fractional-order resonant devices and a differential voltage-current transconductor based on a fractional-order Butterworth low-pass filter, fully demonstrating and highlighting the advantages of Butterworth filters of different orders in terms of amplitude flatness and performance stability [5]. Nonetheless, the majority of the currently available research revolves around the enhancement of single filters or their peculiarities in terms of the frequency domain. Relatively limited comparative research on first-order, second-order, and fourth-order low-pass filters at the system level in a complete AM synchronous demodulation system and their trade-offs has not been done. Specifically, not many studies consider simultaneously various performance measures, including accuracy of gain, delay of phase, noise suppression, and distortion, under the same conditions of work. Without thorough and well-organized comparisons, there is no clear way to define which particular benefits and disadvantages are related to the use of various filter orders in practice.

The whole AM synchronization demodulation system is adopted in this paper. Butterworth low-pass filters of first, second, and fourth order are systematically compared in the same conditions using additive white noise and pink noise. Several performance measures are considered to bring out filter-order trade-offs. This is aimed at giving a clear comparative insight as well as an effective guide to the selection of filters in AM demodulation systems.

2 Materials and Methods

2.1 System Architecture and Simulation Framework

The project explored the workings of low-pass filters of various orders in an amplitude modulation (AM) synchronous demodulation system. In MATLAB/ Simulink, a transmission system was built last in order to guarantee the controllability and repeatability of the environment under evaluation. The system was composed of base signal generation, carrier modulation, addition of noise, modulation of an amplitude phase loop(PPL), low-pass filtering, and quantification of the performance.

In order to make the simulation system more representative of the real conditions of operation, the carrier frequency will be adjusted to 570 kHz in the standard medium wave AM band of operation. A typical narrowband signal is the 1 kHz single-tone sinusoidal signal, which is the baseband message. The sampling rate is set to 5 MHz, much higher than the carrier and noise bandwidth, such that spectral representation can be made accurate and aliasing effects can be avoided.

In order to be fair and compare performances, three low-pass filters are parallelized at the demodulated output: first-order, second-order Butterworth, and fourth-order Butterworth. The cutoff frequency of all filters is identical (2 kHz) and can be used to preserve the baseband signal, attenuate any high-frequency signal, such as carrier leakage and demodulating noise.

2.2 Baseband Signal Generation

The RC Venn bridge oscillator model produces the baseband signal, which produces a stabilized sine wave. The RC Venn bridge oscillator. This is a sinusoidal signal produced by frequency-selective positive feedback. Venn bridge network. This architecture consists of parallel and series RC branching, and offers zero phase shift and $\frac{1}{3}$ attenuation at resonant frequency $f_0=\frac{1}{2\pi RC}$. The amplifier gain is adjusted to about 3 in order to keep the amplitude at the Barkhausen criterion. Automatic gain control is often implemented using nonlinear components in the feedback path to maintain the amplitude of the output and to remove distortion. The reason why this type of oscillator was selected is due to its precise oscillation frequency and excellent amplitude control with nonlinear gain control.

The feedback transfer function of the frequency-selective RC network is defined as shown in Equation (1). For a symmetric Wien bridge configuration with $R_1=R_2=R$ and $C_1=C_2=C$, the feedback factor can be expressed as

$$\beta_{(s)}=\frac{sRC}{s^2R^2C^2+3sRC+1} \tag{1}$$

Here, β(s) denotes the feedback transfer function of the frequency-selective RC network in the Wien bridge oscillator, where s is the Laplace variable. The parameters R and C represent the resistance and capacitance of the symmetric RC network, respectively. In this study, the component values are chosen as R=15.9 kΩR and C=10 nFC, resulting in an oscillation frequency of approximately 1 kHz.

The frequency of oscillation is calculated as the product of the RC time constant, and the nominal frequency of oscillation of the selected values is approximately 1 kHz. In a typical startup, the amplifier gain is adjusted somewhat higher than the theoretical limit to achieve oscillation, and once in the steady state, the gain reduction with the reverse diode in the feedback circuit can be used to control the feedback. In this way, it is possible to obtain a low-distortion sine wave with constant amplitude.

To facilitate theoretical analysis, signals are normalized by their steady-state peak amplitude. This normalized baseband signal will subsequently be used in the analytical derivation of the demodulation gain and error metrics.

2.3 AM Modulation and Channel Noise Modeling

Amplitude modulation is implemented by direct multiplication. A unit amplitude sinusoidal carrier at frequency 570 kHz is multiplied with the normalized baseband signal, resulting in a conventional double-sideband AM waveform with carrier. The mathematical representation of the modulated signal is given in Equation (2). The carrier is modeled as a unit-amplitude sinusoid at angular frequency ω_c, while the baseband message is normalized to avoid over-modulation.

$$s(t) = [1+m_n(t)]\sin(\omega_c t+\phi_c) \quad (2)$$

Here, s(t) represents the amplitude-modulated signal, $m_n(t)$ denotes the normalized baseband message signal, and $\omega_c=2\pi fc$ is the angular frequency of the carrier. The carrier frequency is set to f_c=570 kHz, and ϕ_c denotes the initial carrier phase, which is assumed to be constant.

Noise following the modulation is to simulate the actual conditions of transmission. There are two kinds of noise: white noise and pink noise. White noise includes wideband thermal noise and electronic noise, whereas pink noise is the low-frequency predominant interference that is prevalent in electronic systems and natural settings.

The pink noise is created by the Voss algorithm, a combination of various random processes that have varying scaling rates to create a signal that has a power spectral density (PSD) that is inversely proportional to frequency. Spectral analysis is used to confirm the spectral properties of the noise generated, and the findings are shown in Fig. 1. Plotting noise PSD against frequency in dBm (y-axis) vs. frequency in MHz (x-axis) on a log scale (Fig. 1), the curve depicted here is of the expected 1/f behaviour, and while there are slight random deviations in the high frequency portion, this is in line with the noise stochastic properties.

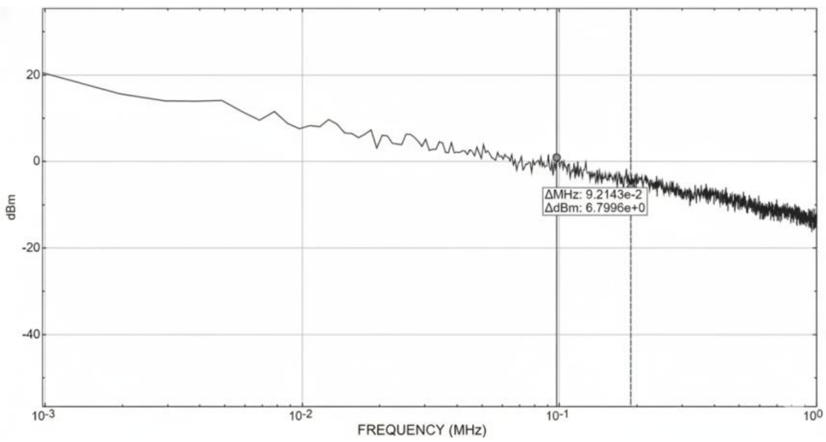

Fig. 1. Power spectral density curve of pink noise generated by the Voss algorithm (Photo/Picture credit: Original).

White noise was created with the help of the standard random number generator that produces a signal with a uniform power spectral density (PSD) over the whole spectra. Spectral analysis of the noise generated was used to verify their spectral properties and the data was plotted in Fig. 2. Fig. 2 plots the plots regarding noise PSD (dBm) (y-axis) and frequency (MHz) (x-axis) on a logarithmic scale, the curves observed here are predicted as anticipated: the PSD remains relatively constant over the whole range of frequencies, and the large random variations in the high-frequency band are typical of random noise.

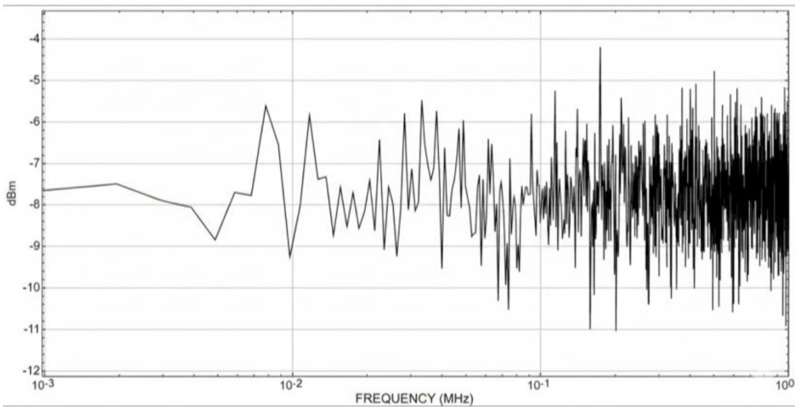

Fig. 2. Power spectral density curve of white noise generated by the Voss algorithm (Photo/Picture credit: Original).

2.4 Synchronous Demodulation Using PLL

The carrier signal multiplies with the received signal in the demodulator, and the carrier is phase-locked to the input signal by a PLL. The PLL makes certain that the frequencies and phases are synchronized with each other, and in essence, it stifles demodulation errors that occur due to carrier mismatch. The multiplier output has the baseband signal component and high-frequency components centered around twice the carrier frequency.

Using trigonometrical identities, it can be said that the demodulated signal is a low-frequency signal that is proportional to the original signal and the high-frequency signal, which has to be filtered off. This derivation can be summed up in Equation (3).

$$u(t)=\frac{1}{2}[1+m_n(t)]\left[\cos(\theta_e(t))-\cos(\theta_c(t)+\hat{\theta}(t))\right] \tag{3}$$

Here, u(t) is the output of the synchronous multiplier. The term $\theta_c(t)=\omega_c t+\phi_c$ represents the instantaneous phase of the received carrier, whereas $\hat{\theta}(t)$ indicates the angular velocity of the domestically produced oscillator under the influence of the phase-locked loop. Phase error is given by $\theta_c(t)= \theta_c(t) - \hat{\theta}(t)$. When the locked condition $\theta_e(t)$ has a low value, the global mean level is zero, and a low-frequency signal of the same magnitude as the underlying baseband signal is obtained, with a high-frequency signal centred at twice the carrier frequency.

2.5 Low-Pass Filter Design and Characteristics

In order to estimate how various filtering properties affect the demodulation performance, this paper conducted an experiment where three low-pass filters are implemented yet varying in order and their frequency response properties; they all have a cutoff frequency of 2 kHz.

The first-order low-pass filter is simple to implement and has linear phase characteristics, but its stopband attenuation is limited. Its transfer function is given in Equation (4).

$$H_1(s)=\frac{\omega_0}{s+\omega_0}=\frac{1}{\tau s+1} \tag{4}$$

Here, $H_1(s)$ denotes the transfer function of the first-order low-pass filter, and $\omega_0=2\pi f_{LP}$ is the cutoff angular frequency. In this work, the cutoff frequency is chosen as f_{LP}=2 kHz, which is sufficient to preserve the 1 kHz baseband signal while attenuating higher-frequency components.

The second-order Butterworth filter maintains a maximally flat passband response while exhibiting a steeper roll-off characteristic. Its transfer function is given in Equation (5).

$$H_2(s)=\frac{\omega_0^2}{s^2+\sqrt{2}\omega_0 s+\omega_0^2} \tag{5}$$

Here, $H_2(s)$ represents the transfer function of the second-order Butterworth low-pass filter. The parameter ω_0 denotes the cutoff angular frequency, which is identical to that used in the first-order filter. The coefficient $\sqrt{2}$ arises from the Butterworth polynomial, ensuring a maximally flat magnitude response in the passband.

The fourth-order Butterworth filter further improves the steepness of the transition band and high-frequency rejection capabilities, but it also introduces greater phase delay and higher implementation complexity.

$$H_4(s)=\frac{\omega_0^4}{s^4+2.6131\omega_0 s^3+3.4142\omega_0^2 s^2+2.6131\omega_0^3 s+\omega_0^4} \tag{5}$$

Here, $H_4(s)$ denotes the transfer function of the fourth-order Butterworth low-pass filter. The coefficients of the denominator polynomial correspond to the standard fourth-order Butterworth response, providing a steep roll-off and strong high-frequency attenuation. The cutoff angular frequency ω_0 is identical to that used in Equations (4) and (5), ensuring a fair comparison among filters of different orders.

The theoretical phase delay of each filter at the message frequency is calculated based on its phase response, for subsequent comparison and verification with simulation results.

2.6 Performance Metrics and Data Processing

The steady-state data will be extracted from the simulation, and the following indicators will be calculated: demodulation gain, phase delay time (PDT), signal-to-noise ratio (SNR), carrier rejection ratio (CSR), total harmonic distortion (THD), and steady-state error.

The demodulation gain is defined as the ratio of the peak output signal to the peak input signal at 1 kHz, and theoretically should be proportional to the filter's amplitude response at that frequency. PDT is a core indicator characterizing the phase tracking accuracy and phase response linearity of the system at the message signal frequency, and is directly calculated from the phase response at the target frequency. SNR, CSR, and THD reflect the system's noise immunity, modulation spectral purity, and nonlinear distortion level, respectively, all obtained through spectral analysis based on Fast Fourier Transform. Simultaneously, the steady-state error is determined using a least-squares sine fitting method; this error is an indicator of the system's steady-state tracking accuracy to an ideal sinusoidal input.

3 Results

3.1 Time-Domain Results

The time-domain performance of the AM synchronous demodulation system was evaluated using the steady-state waveform obtained by removing the startup interval (0–0.01 seconds) associated with the Wien bridge oscillator.

Then the three filters were able to recover the signal at 1 kHz by the process of synchronous demodulation followed by low-pass filtering. There was, however, a large difference between the smoothness of the waveforms and the relative phase delay.

Fig. 3 presents the time-domain signal waveforms of the modulated and demodulated signals of the three filters. The x-axis shows the time in seconds, whereas the y-axis indicates the amplitude. The findings indicate that the residual ripple and high-frequency swings are still present and, therefore, the stopband attenuation is not that high. Conversely, there is a tremendous increase in smoothness in the output when fourth-order Butterworth and second-order Butterworth filters are applied.

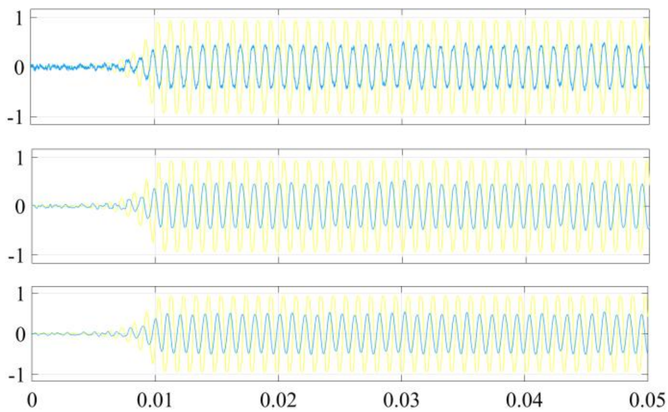

Fig. 3. Comparison between the waveform filtered by three types of filters and the original waveform (Photo/Picture credit: Original).

Based on looking at the time-domain waveforms, the fourth-order Butterworth filter gives the smoothest and clearest output, although it additionally introduces the biggest phase delay. The delay generated by the first-order filter is the lowest, and the second-order filter is in between. The phase delay also has a monotonic rising curve as the filter order is increased, which is as expected by theory, as more group delay is expected to be present in higher-order low-pass filters.

3.2 Frequency-Domain Results

According to the amount of power spectral density estimation of the demodulated signal, analysis of the frequency domain properties of the system is possible. The demodulated signal, before undergoing low-pass filtering, still has large high-frequency signal components as well as the baseband component, and a visible residual carrier element can be seen at 570 kHz.

Fig. 4 displays the power spectral density of the signal at different conditions of filtering. The frequency is drawn on the x-axis on a logarithmic scale, and the power on the y-axis. The Fig. represents four curves, which are the output of the unfiltered signal and three low-pass filters, respectively. There is a distinct peak of all curves at 1 kHz. The high-frequency components of the curves are quite different: the unfiltered signal (yellow) is relatively flat at high frequencies, where there is a peak at about 570 kHz, whereas the filtered signals (blue, orange, and green) are gradual decreases of power, with the green curve having the slowest attenuation.

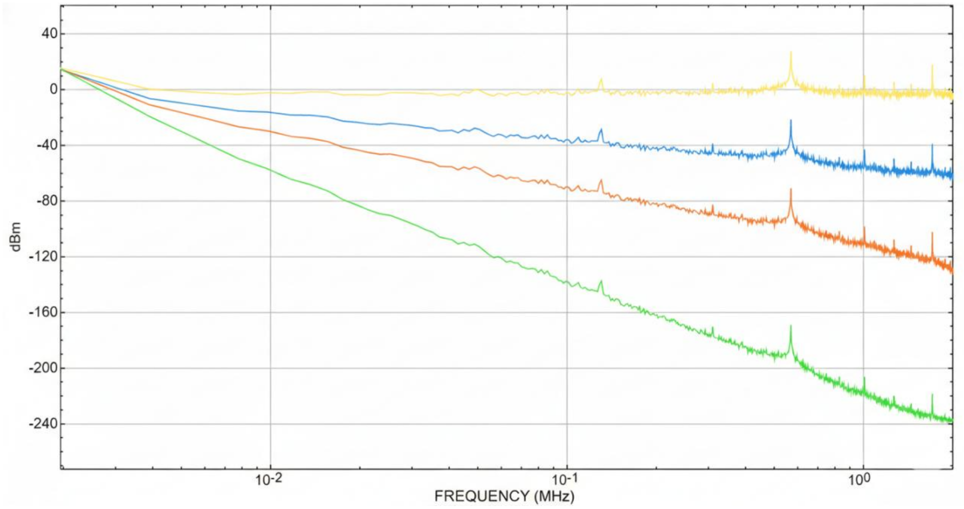

Fig. 4. Comparison of Signal Spectrum Under Different-Order Low-Pass Filters: Original vs. Filtered Outputs (Photo/Picture credit: Original).

3.3 Quantitative Performance Metrics

To be able to quantitatively compare them, this paper considered the following key performance indicators, which are present demodulation gain, PDT, SNR, CSR, THD, and steady-state error. When calculating all the indicators, steady-state data were used so as to achieve a consistent result. Table 1 summarises the final results.

Table1. Performance comparison of three types of filters

Error / Filter	Gain	PDT	SNR	CSR	THD	err
First-order filter	0.448	0.0004791	42.7	-46.86	-29.4	0.02433
Second-order filter	0.4831	0.0005405	50.53	-95.34	-31.09	0.02161
Four-order Butterworth filter	0.463	0.000623	54.3	-107.8	-32.22	0.01348

The outcomes of the simulation indicate that filter order is one of the important parameters that influence the general performance of the AM synchronous demodulation system. Butterworth filters of higher-order are able to obtain better out-of-band noise reduction, carrier leakage reduction, and signal spectral purity, whereas Butterworth filters of lower-order can be used with lower phase delay, and fewer hardware and algorithm requirements. The Butterworth 2 rd filter is a compromise between demodulation and the complexity of system implementation. A fourth-order Butterworth filter is a better choice in a system where noise and carrier leakage suppression are an extreme requirement.

3.4 Summary of Results

The findings of this paper affirm that the arrangement of a low-pass filter is a determining factor in the total performance of an AM synchronous demodulation system. The results of all the tested filters were capable of effectively recovering the baseband signal, but major differences were seen in the main performance features in terms of the noise suppression capability, carrier suppression effect, and characteristics of phase delay among the various filters. This finding is quite consistent with the theory of classical design of filters as well as the aspects of coherent demodulation methods.

The higher-order Butterworth filters are purer in high frequencies due to steeper attenuation curves. The experiments have demonstrated that the Butterworth filter of fourth-order can be used to reduce leftover carrier and high-frequency noise with high efficiency, thus enhancing SNR and CSR. The same tendencies are observed by the other available studies of synchronous detection systems, in which better low-pass filtering can greatly increase the accuracy of demodulation in a noisy case [6]. This good performance, however, comes with a higher phase delay that can disadvantage the system performance in areas where a quick transient response is required.

The Butterworth filters of the second order provide a great trade-off between frequency selectivity and phase delay. Their maximally flat passband property results in a minimum amplitude distortion and gives adequate attenuation to undesired spectral content. This trade-off concurs with results on the optimization of filters in communication receivers, and in realistic engineering applications, filters of moderate order tendentially preferred [7]. First-order low-pass filters are simple in form and have a small phase delay, but they have a low attenuation factor against carrier leakage that prevents them from being employed in high-performance demodulation systems.

In addition, the effective demodulation gain of higher-order filters also showed a slight reduction during the experiment. This can be explained by the fact that more phase alignment errors are being sensed by a larger group delay, and this is a mechanism that is in conformity with the findings made with reference to coherent demodulators and PLL [8].

To take it even further, it is important to mention that any of the results in this work is obtained through the use of simulation experiments in a controlled setting, and its practicality must be an even more important aspect that must be confirmed in the context of practical engineering operations [9, 10].

4 Conclusion

Systematic comparison. This paper compares the performance of first-order, second-order, and fourth-order low-pass filters in AM synchronous demodulation systems under the same conditions of the simulation. A fair performance evaluation was reached by building a modulation-demodulation framework in whole such as carrier synchronization, noise modeling, and parallel filtering. The findings show that the filter order has a profound effect on the demodulation quality, especially in the following specifics: noise suppression, carrier suppression, phase delay, and signal distortion.

It has been demonstrated by simulation that higher-order Butterworth filters are more capable of suppressing out-of-band noise and residual carriers and, because of these, enhance SNR and CSR and reduce overall harmonic distortion THD. This is, however, at the expense of a larger phase delay and a little lower demodulation gain. The benefit of the first-order filters is that they do not cause much phase delay and are not complex in their structure, but do not have many capabilities of suppression. The second-order filters have a good balance between performance and complexity, and hence they are suitable in most practical systems.

Another limitation inherent in this study is that all the results are derived on the basis of an ideal simulation without having to take non-ideal considerations like component tolerances and phase noise. The next task in the field of work may be the hardware implementation or may involve the real conditions of the system, so as to better verify the conclusions.

An AM synchronous demodulation and optimized low-pass filter demodulation are still useful in low-cost radio receivers, Internet of Things communication links, and signal measurement systems. With further development of communication systems into system designs that are energy-saving and resource-constrained, the order of the filters discussed in this work will also be relevant in the optimization of the receivers and system-level designs in communication systems in the future.

References

[1] Jia, Y., Ni, M. H., Wu, M. Y., Qin, F. H., & Liu, M. Z.: Design of an orthogonal amplitude modulation and demodulation communication experiment system based on LabVIEW. Shiyan Kexue yu Jishu/Experiment Science and Technology. 19(5), pp. 25-30 (2021)

[2] Jiménez-Zacarías, L. L., & Campos-Cantón, I.: Lorenz system manufacturing with a Butterworth filter. Integration. 103, pp. 102386 (2025)

[3] Liu, W., Zhang, L. Y., & Zhou, Z.: Ultra-wideband pulse amplitude modulation and its frequency-domain correlation demodulation. Journal of Beijing University of Posts and Telecommunications. 30(4), pp. 1-5 (2007)

[4] Li, H., Gao, Y., Guo, X., & Ou, S.: Variable projection order Ekblom norm-promoted adaptive algorithm, VPO-EPAA. Journal of Shandong University of Science and Technology (Natural Science). 44(4), pp. 1-10 (2025)

[5] Krishna, B. T., & Mithunchakkaravarthy, M.: A comparative study on the implementation of fractional order Butterworth lowpass filter using differential voltage current conveyor. International Journal of Circuits, Systems and Signal Processing. 17, pp. 136-142 (2023)

[6] Wu, L., Zhao, G., & Feng, Z.: A high resolution synchronous demodulation method based on gated integrator for precision sensors. IEEE Transactions on Instrumentation and Measurement. 71, pp. 9504009 (2022)

[7] Kennedy, H. L.: Lecture notes on the design of low-pass digital filters with wireless-communication applications (Version 2). arXiv. pp. 1-15 (2022)

[8] Chang, J., Zhu, M., Duan, R., Wang, X., & Wang, M.: Phase demodulation for distributed acoustic sensing based on improved phase-locked loop. IEEE Transactions on Instrumentation and Measurement. 75, pp. 6501216 (2026)

[9] Li, H., Zhang, X., & Gong, H.: Optimization design of FIR digital filter based on frequency sampling method. Information Technology. 2026(3), pp. 8 (2026)
[10] Huang, W., He, S., & Wen, C.: Equivalence of Kalman filtering and least squares for correlated noise systems. Information Technology. 2025(5), pp. 53 (2025)